HT2019-3403

PROTOTYPE RESULTS FOR A SALT HYDRATE PCM THERMAL ENERGY STORAGE SYSTEM

Sean H. Hoenig
Advanced Cooling Technologies, Inc.
Lancaster, PA, USA

Richard W. Bonner III
Advanced Cooling Technologies, Inc.
Lancaster, PA, USA

Joshua M. Charles
Lehigh University
Bethlehem, PA, USA

Chien-Hua Chen
Advanced Cooling Technologies, Inc.
Lancaster, PA, USA

Fangyu Cao
Advanced Cooling Technologies, Inc.
Lancaster, PA, USA

ABSTRACT

Air-cooled condenser systems incur a high cost of operation during peak power demand due to hot ambient temperatures, resulting in poor thermal performance. To shift the thermal performance of air-cooled condenser systems closer to that of wet cooling towers, a salt hydrate phase change material (PCM)-based supplemental thermal energy storage system is proposed. Low-grade waste heat from saturated steam in a power generation cycle is stored in a "cold" sink of PCM during the day and rejected at night during cooler ambient air temperatures. Passive loop thermosyphons are used to transfer heat in and out of the PCM heat exchanger. A 30MJ prototype was designed, fabricated, and tested to demonstrate the longevity of the system. Repeated thermal cycling tests have been completed for 50 cycles. The measured latent heat capacity results have shown that the salt hydrate solution segregates into different hydration levels over time but can stabilize by remixing the bulk solution.

INTRODUCTION

The effective thermal dissipation of low-grade heat is paramount to the future of the electric power generation industry. A limited supply of cooling water coupled with fractional increases in its cost have left utilities in search of advanced cooling technologies. To combat this issue, the ARPA-e ARID Program sought transformative power plant cooling technologies "that enable high thermal-to-electric energy conversion efficiency with zero net water dissipation to the atmosphere" [1]. One aspect of this program investigated novel supplemental thermal storage mediums for use with air-cooled condenser (ACC) systems. With only 1% of the electric power generation market using dry cooling systems [2], low-cost thermal storage would help offset its inherent inefficiencies during hot ambient temperatures. The main idea is to maintain a "cold" heat sink during the day to maintain high thermal performance, while at night the heat is dissipated to cooler ambient temperatures.

For the ARPA-e program, Advanced Cooling Technologies, Inc., along with Lehigh University and the University of Missouri, proposed a supplemental salt hydrate thermal energy storage system that utilizes an integrated loop thermosyphon-PCM heat exchanger. The thermal energy storage system is located downstream of the air-cooled condenser to supplement cooling of the process steam. This is can be seen in Figure 1.
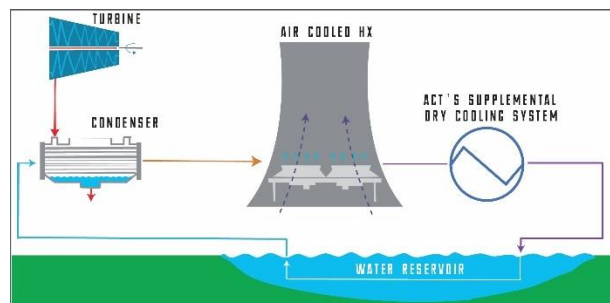

Figure 1. Indirect dry cooling process diagram with a supplemental thermal energy storage system.

In this program, an abundance of research was completed to develop the salt hydrate PCM, primarily by drop calorimetry, thermal cycling, and accelerated corrosion tests [3, 4]. The 30MJ prototype system is a culmination of these efforts to increase the technology readiness level of the salt hydrate PCM and evaluate the long-term use of the thermal storage medium. The prototype utilizes loop thermosyphons to transfer heat in and out of the PCM reservoir. The salt hydrate solution is a calcium chloride hexahydrate ($CaCl_2 \cdot 6H_2O$) mixture, consisting of additives to suppress subcooling and prevent phase segregation. As seen in Figure 2, the prototype system consists of a steam evaporator, PCM heat exchanger, and air-cooled radiator to model an indirect dry cooling system.
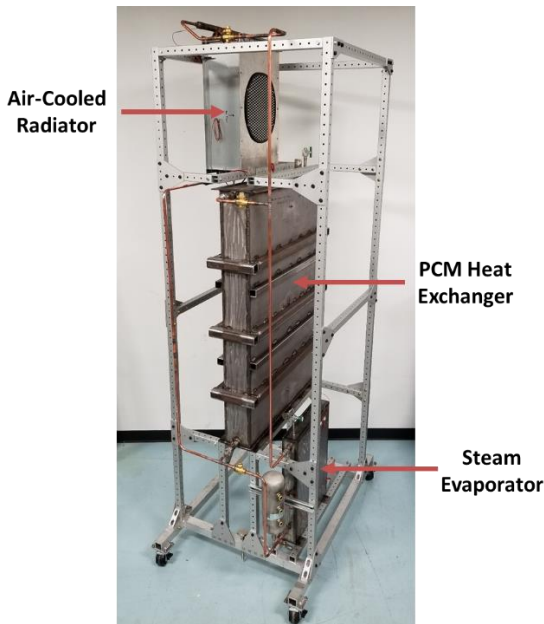

Figure 2. 30MJ latent heat capacity heat exchanger prototype system designed and fabricated by ACT.

The apparent benefits of salt hydrate PCM are well noted. While the relatively low-cost and high latent heat capacity of salt hydrates is preferable, the reduction of phase separation during thermal cycling is unsolved [5]. Additionally, the low thermal conductivity of salt hydrates warrants the use of heat pipes for high heat transfer efficiency into the PCM [6]. While there have been noteworthy efforts to model these physical effects with low computational power [7, 8, 9], this effort will specifically demonstrate the long-term use of the aforementioned salt hydrate solution in an experimental prototype. Fundamental design analysis was completed to ensure the thermal performance of the prototype met the program goals of a 10-hour melt time. Following qualification of the system, accelerated thermal cycling tests were completed for 50 cycles.

EXPERIMENT

In order to test the prototype system, the salt hydrate solution needed to be synthesized at bulk scale. To make 225kg of PCM solution, a custom charging station was designed and fabricated to mix the components and charge the heat exchanger.

This setup can be seen in Figure 3. A stainless steel mixing paddle was connected to an agitator motor. With the proprietary weight percent of the PCM components placed into the drum, the solution was well mixed. Table 1 demonstrates the specific components used. After mixing, the solution was placed in a walk-in freezer to solidify the components and subsequently was melted using a drum heater. This was completed to then remove any excess water used in the synthesis process. To charge the PCM solution in the heat exchanger, a vacuum pump was used to decrease the pressure inside the heat exchanger. A series of valves were used to control the flow of PCM into the internal heat exchanger volume. To maintain positive pressure, dry nitrogen gas was pumped inside the drum during this process.
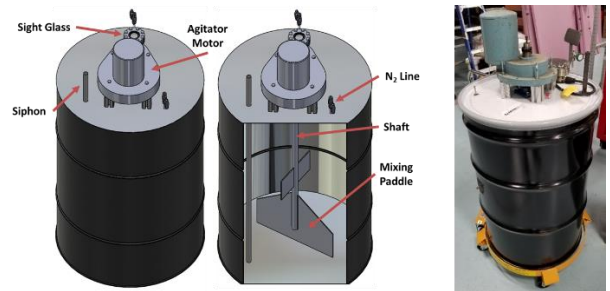

Figure 3. Designed PCM charging station used to synthesize the bulk PCM solution for the heat exchanger.

Table 1. PCM components

Name	Chemical Formula	Industrial Product	Function
Anhydrous Calcium Chloride	$CaCl_2$	BRINERS CHOICE	Salt
Deionized Water	H_2O	In-House Filter	Hydrate
Strontium Chloride Hexahydrate	$SrCl_2 \cdot 6H_2O$	Barium & Chemicals	Subcooling Suppression
Potassium Chloride	KCl	Alfa Aesar	Phase Segregation

With the heat exchanger fully charged with PCM, testing of the system could now ensue. Thermal cycling tests were completed by melting the PCM to a 100% melt fraction with additional superheating above the melt range of 26-27°C. Following this effort, a solidification cycle was completed with additional supercooling below its melt point. As demonstrated below in Figure 4, during the melt cycle, heat is generated in a steam evaporator via electric cartridge heaters. This heat is transferred into the loop thermosyphon and its working fluid (R-134A) to generate two-phase flow. The R-134A condenses along the internal tubing of the heat exchanger, transferring heat into the PCM solution to melt it. A Yokogawa power analyzer integrated the total electrical energy input to determine the overall energy storage capacity of the system. Thermocouples were placed inside the PCM heat exchanger to measure the PCM temperature. During the solidification cycle, heat is removed by an air-cooled radiator using the loop thermosyphon. A series of valves orients the loop thermosyphon for each cycle to function as intended, as demonstrated in Figure 4. Otherwise, the system

is considered a passive heat transfer device. This thermal cycling was repeated for 50 cycles in order to learn more about the long-term use of this PCM solution for thermal energy storage.
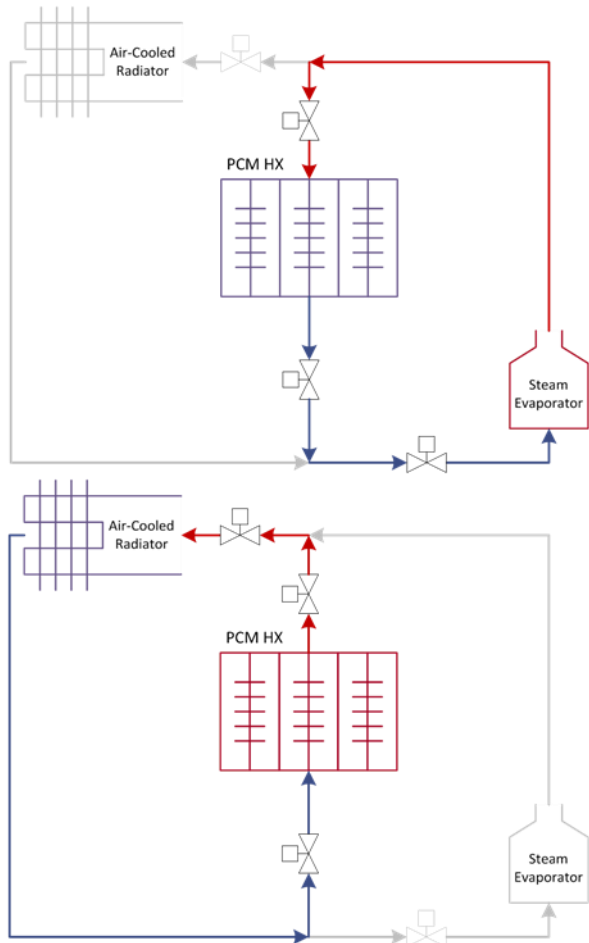

Figure 4. Process flow diagrams for the melting (top) and freezing (bottom) cycles of the prototype system.

RESULTS

In order to qualify the prototype 30MJ thermal energy storage system, results from a finite element analysis (FEA) of the system was compared with experimental test results. The FEA simulation was created in Autodesk with a symmetrical portion of the internal heat exchanger volume. A boundary condition of 40°C steam was used to simulate the heat source of power plant generators. An initial condition for the solid PCM was set to 25°C, which is right below the melt range of 26-27°C. The PCM properties of the salt hydrate mixture were input into the program based on the calorimetry and DSC testing completed by Lehigh. An effective heat transfer coefficient was used at the tube wall to lump together the resistances in series upstream of the PCM heat exchanger. This value was approximately $h_e = 300$ W/m²-K. The experimental test was completed with equivalent boundary and initial conditions, as described previously. The results are seen in Figure 5. For this melt test, the instantaneous power and accumulated energy curves were plotted against time for both the experiment and simulation. The model demonstrates

that the PCM melts in approximately 11.5 hours and subsequently superheats. This is clearly seen as the power input curve drops off due to the change in PCM properties to specific heating (superheating) from latent heating (melting). For the experimental test, with a known mass of PCM in the heat exchanger (225kg), the total energy storage capacity due to melting of the PCM is 8.4kWh. The experimental test is therefore fully melted in approximately 10.5 hours. The experimental and simulated thermal performance results matched within 10%, which was acceptable for these tests.
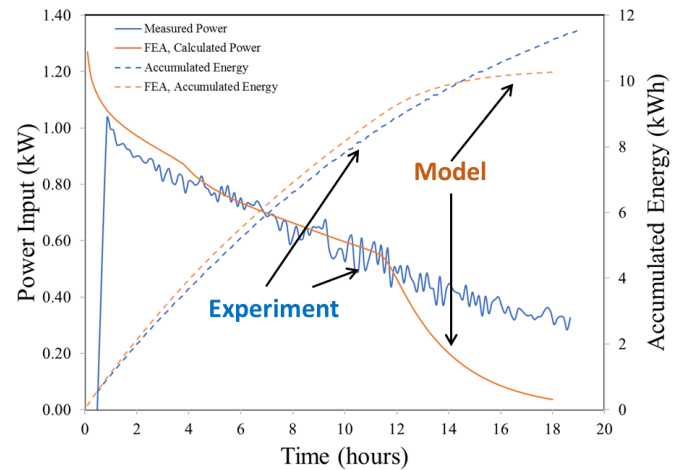

Figure 5. Experimental thermal performance match FEA results within 10% for equivalent boundary and initial conditions.

The results of the thermal cycling tests are discussed in the next several paragraphs. Note that these are accelerated tests, compared with the original goals, such that the melt test is completed within an 8-hour work day, while the freeze test occurs overnight. Second, the final results are presented in terms of a calculated latent heat capacity term. Due to the fact that the latent heat capacity is normally constant, this provides insight into the long-term stability of the salt hydrate PCM. Then, the results are further analyzed to demonstrate additional evidence of segregation. Fifty total cycles were completed, where one complete cycle is defined as consisting of both a melt and a freeze test. Equation 1 was used to calculate the latent heat capacity for the melt test of each cycle. The total energy input is determined using the power analyzer results. The mass of PCM was measured to be 225kg when the heat exchanger was charged. The melt range was assumed to be 26-27°C, based on calorimetry and DSC results. Since the temperature of the metal portions of the heat exchanger were not directly measured, it was assumed that there was a 10°C change in temperature of the metal for all calculations. This assumption was made in reference to the observed change in PCM temperature for the test. To measure PCM temperature, three thermocouples were placed at different locations along the z-axis (height) of the heat exchanger. The results below in Figure 6 are the average calculated latent heat capacity from these three measurements. Figure 7 contains the individual latent heat capacity results from each thermocouple measurement.

$$L_f = \frac{Q_{total} - m_{pcm}c_{p,s}(T_{m,i}-T_i) - m_{pcm}c_{p,l}(T_f-T_{m,f}) - m_m c_{p,m}(T_f-T_i)}{m_{pcm}} \quad (1)$$

The most evident result from these figures is that there are two distinct sections in the thermal cycling tests. The first 30 cycles exhibited no change in test conditions, but demonstrated approximately a 10% degradation in latent heat capacity. This noticeable change in performance was simultaneously demonstrated on a small scale with similarly prepared laboratory grade components of the salt hydrate solution [4]. To alleviate this issue, it was theorized that the hexahydrate crystals needed to be reformed via mixing. Over time, a portion of the hexahydrate crystals covert to tetrahydrate crystals as the tetrahydrate phase is preferentially formed over a narrow temperature range during each freezing cycle. As seen in Table 2, calcium chloride tetrahydrate is denser, has a lower latent heat capacity, and a higher melt point than calcium chloride hexahydrate. Thus, the segregated tetrahydrate sinks to the bottom of the heat exchanger, generating additional thermal resistance and a smaller calculated latent heat capacity for the PCM. After the 30th cycle, the salt hydrate solution was heated until the tetrahydrate melt temperature was exceeded, allowing the tetrahydrate to mix with liberated water molecules. This created re-formed hexahydrate crystals. This took approximately 24 hours. This mixing stabilized the calculated latent heat capacity term during subsequent thermal cycling tests. It is clear that the difference in data trends between section 1 and 2 implies that mixing reforms the hexahydrate crystals, improving long-term stability. This is the main conclusion of this experiment test without additional data beyond 50 total cycles. Although the latent heat capacity values are lower by approximately 15% than what is expected from the differential scanning calorimetry (DSC) results (134 kJ/kg), this is acceptable for a more imprecise calorimetry technique. The trend of the initial degradation and subsequent stabilization of the latent heat capacity term is promising for long-term use.
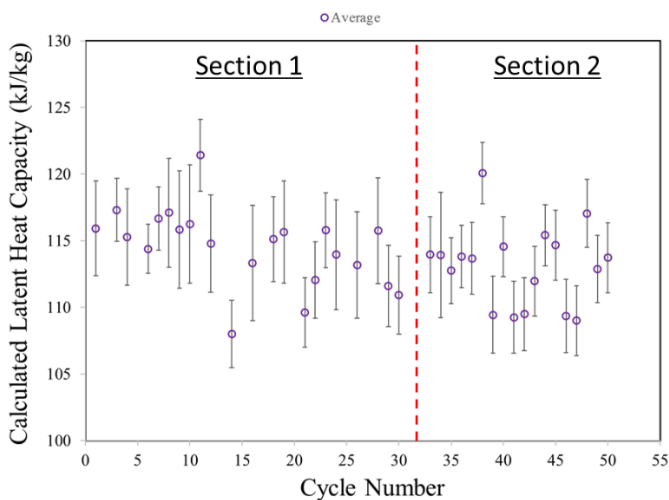

Figure 6. Average latent heat capacity for each thermal cycle.

Additional insight into Figure 7 concerns the variability of the data for the bottom thermocouple compared to the middle and top thermocouples. It is well understood that due to the design of the heat exchanger, the lowest thermal resistance pathway is at the top of the heat exchanger. This portion of the system is where saturated refrigerant vapor initially condenses along the internal heat exchanger tubes. As more heat is transferred into the PCM, more condensate forms and accumulates. This leads to a build-up of a liquid pool of refrigerant, which contributes to variability of the data for the bottom thermocouple. The middle and top thermocouple results do not demonstrate this variability for the aforementioned reasons. The important point is that the trend in the results for each thermocouple is the same for each section of the thermal cycling tests.
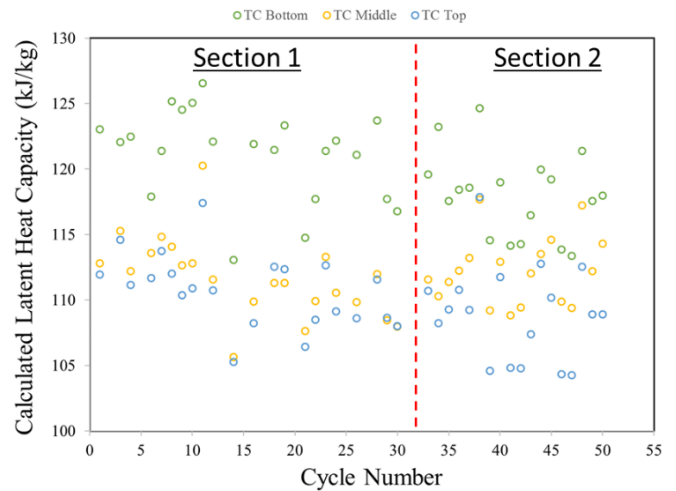

Figure 7. Individual latent heat capacity for each thermal cycle for each thermocouple measurement.

Table 2. PCM properties [10, 11]

	Melt Point (°C)	L_f (kJ/kg)	ρ (kg/m^3)
CaCl$_2$·6H$_2$O	29°C	170-192 kJ/kg	1712 kg/m^3
CaCl$_2$·4H$_2$O	39°C	158 kJ/kg	1826 kg/m^3

The results presented in Figure 8 and Figure 9 further indicate the phase segregation results determined in section 1 of the thermal cycling tests. In Figure 8, the instantaneous power curve for the 30th cycle decreased. Consequently, it took longer for the PCM solution to melt and reach the same energy storage capacity as during the 1st cycle. When the PCM temperature measurements were analyzed in Figure 9, the melt curves increased in all thermocouple locations. Calcium chloride tetrahydrate has a higher melt point, leading to faster heating of the PCM before and after it is fully melted. Additionally, the top and middle thermocouple measurements dramatically increased in temperature compared to the bottom thermocouple measurement. This indicates not only segregation of phase throughout the entire heat exchanger volume but also locally on each heat exchanger fin. Following this insight, the long mixing test took place, leading to the results in Figure 10 and Figure 11. In Figure 10, following the long mixing test, the instantaneous

power curve for the 33rd cycle matched the 1st cycle. The energy storage capacity for both met the 8.4kWh target at virtually the same time. In Figure 11, the melt temperature distributions of the PCM thermocouples also match better between the 1st and 33rd thermal cycles. The temperature distribution curve returns to its original shape. This trend indicates that mixing the salt hydrate solution by fully melting all of the phases helps restore the PCM to its original thermal storage capacity, which allows for long-term use. The trends exhibited in Figure 10 and Figure 11 continued for the duration of the thermal cycling tests. The combination of the aforementioned analysis was used to gain valuable insight into how the salt hydrate solution changed and stabilized throughout the thermal cycling tests.
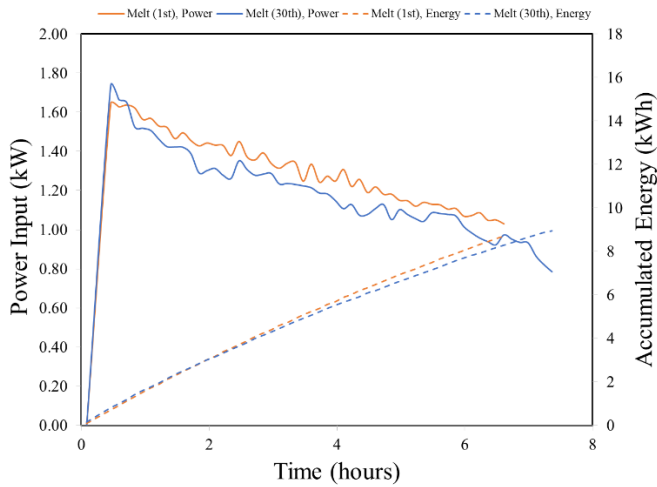

Figure 8. Thermal performance results for the 1st and 30th thermal cycle test.
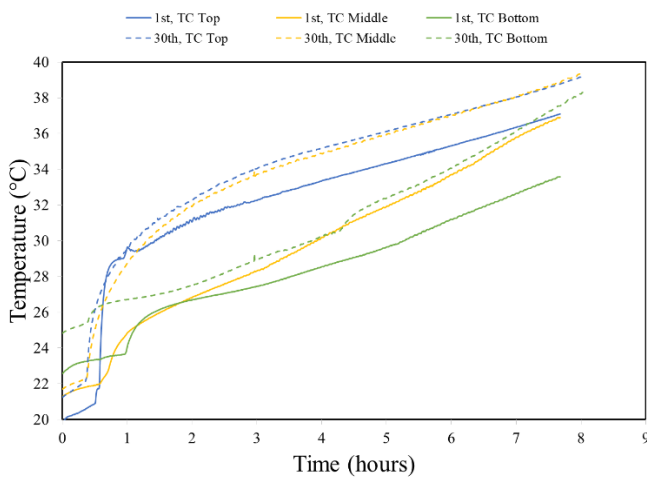

Figure 9. Temperature measurements of the PCM for the 1st and 30th thermal cycle tests.
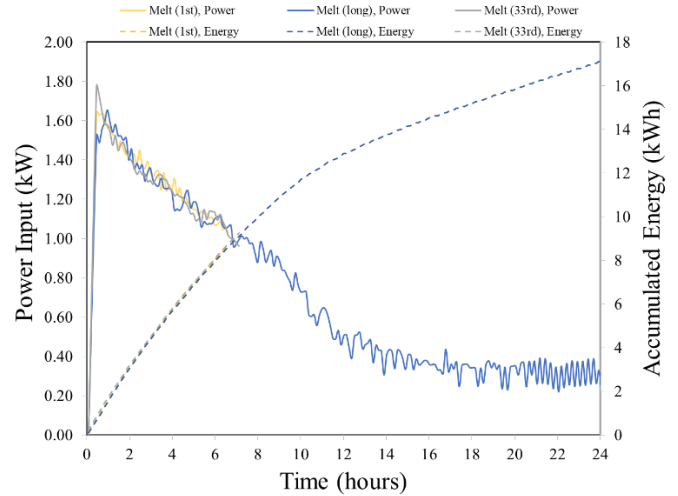

Figure 10. Thermal performance results for the 1st, long, and 33rd thermal cycle tests. The long test is when the PCM was superheated for 24 hours to mix the solution.
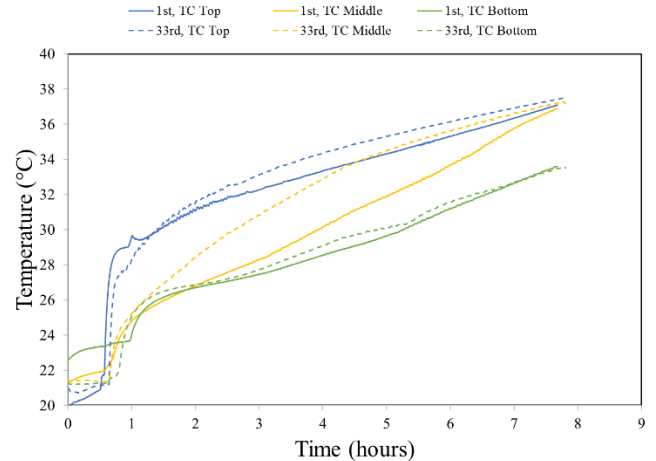

Figure 11. Temperature measurements of the PCM for the 1st and 33rd thermal cycle tests.

To further validate and understand the prototype findings, small scale thermal cycling tests were completed. The same salt hydrate solution used in the prototype system was collected for this additional thermal cycling test. It should be noted that this salt hydrate solution was prepared with 2.89wt% excess water. This additional water was used as part of the PCM synthesis procedure in order to ensure sufficient water was introduced to create hexahydrate crystals. A drop calorimeter was used to determine the precise latent heat capacity of the solution, while a programmable water bath was used to repeatedly melt and freeze the solution. After 40 thermal cycles, the 2.89wt% excess water sample exhibited phase segregation, as evidenced by the comparable decrease in latent heat capacity in Figure 12. These small-scale thermal cycling results are in agreement with the previously discussed prototype system results. In addition, following this test, samples were created using 0wt% excess water using the same PCM materials as previously. As

evidenced in Figure 12, the 0wt% excess water samples exhibited no phase segregation and a higher measured latent heat capacity than the previous work. Through the work by Charles [4], it has been demonstrated that the ternary phase diagram between calcium chloride, water, and potassium chloride puts both the 0wt% and 2.89wt% excess water samples at eutectic points. However, the 0wt% eutectic point sample has a higher melt temperature than the 2.89wt% eutectic point sample. Due to time and budget constraints, the 0wt% excess water PCM solution was not tested in the large-scale prototype. This important difference in the preparation of the salt hydrate solution may key to maintaining its long-term use and is a direction for further research.
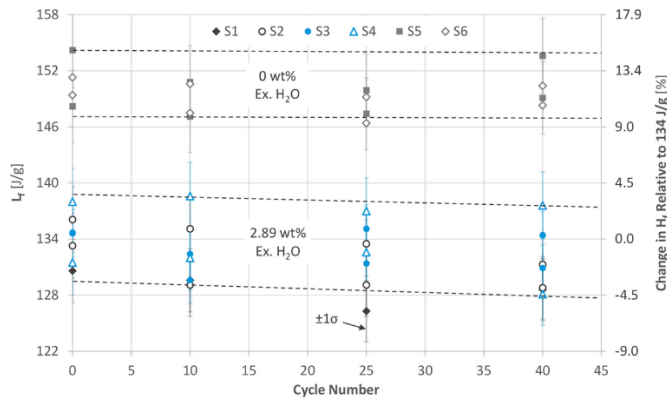

Figure 12. Small scale thermal cycling tests indicate how the preparation procedure dictates long-term stability.

CONCLUSION

A 30MJ latent thermal energy storage system using a salt hydrate solution of calcium chloride hexahydrate with additives was designed and qualified. Fifty thermal cycling tests were completed in order to evaluate the long-term stability of the combined heat exchanger and PCM system. It was determined that this salt hydrate solution undergoes phase segregation due to preferential formation of the tetrahydrate phase over a critical temperature range during crystallization. The incongruent melting and freezing of the salt hydrate solution decreases the latent heat capacity of the PCM over time. Additionally, the salt hydrate solution can be stabilized by fully melting all of the hydration levels present in solution. The 30MJ prototype system itself was a successful demonstration of a passive thermal energy storage unit for daytime storage of waste heat and overnight dissipation of this heat to cooler ambient conditions. Further research is required of the PCM synthesis procedure to validate the long-term stability of the salt hydrate solution. Subsequent use in a pilot scale unit at a power plant will increase the technology readiness level of this thermal energy storage system.

NOMENCLATURE

Subscripts
e: effective
s: solid
l: liquid
pcm: phase change material
i: initial
f: final
m,i: melt range, initial
m,f: melt range, final
m: metal

ACKNOWLEDGEMENT

REFERENCES

[1] *ARPA-e ARID Program Overview*. Retrieved December 28, 2018 from http://arpa-e.energy.gov/, (2014).

[2] U.S. Department of Energy., *The Water-Energy Nexus: Challenges and Opportunities*. Retrieved September 09, 2016 from http://www.energy.gov/, (2014).

[3] Charles, J., Romero, C., Neti, S., et al. "Maximizing Plant Efficiency While Minimizing Water Usage Through Use of a Phase Change Material-Based Cold Energy Storage System". *ASME. ASME Power Conference*, Volume 2: 2017. Doi: 10.1115/POWER2018-7318.

[4] Charles, Joshua M., "Performance and Stability of CaCl$_2$·6H2O-Based Phase Change Materials" *PhD diss.*, Lehigh University, 2018.

[5] Xie, Ning, et al. "Inorganic Salt Hydrate for Thermal Energy Storage" *Appl. Sci.* 2017, 7, 1317; doi: 10.3390/app7121317.

[6] Mohamed, S.A., et al. "A review on current status and challenges of inorganic phase change materials for thermal energy storage systems" Renewable and Sustainable Energy Reviews, 70 (2017) 1072-1089.

[7] Hoenig S., CJ Pan, C.-H. Chen, and R.W. Bonner. "Thermal Resistance Network Model for Heat Pipe – PCM Based Cool Storage System." *2nd Thermal and Fluids Engineering Conference – ASTFE*, April 02-05, 2017, Las Vegas, NV.

[8] Pan, C., Hoenig, S., et al. "Efficient Modeling of Phase Change Material Solidification with Multidimensional Fins" *International Journal of Heat and Mass Transfer*. 115 (2017) 897-909.

[9] Pan, C., Hoenig, S. et al. "Efficient optimization of a longitudinal finned heat pipe structure for a latent thermal energy storage system", *Energy Conversion and Management*, 153 (2017) 93-105.

[10] Sharma, S.D., Kitano, H. and Sagara, K., 2004. Phase change materials for low temperature solar thermal applications. http://www.eng.mie-u.ac.jp/research/activities/29/29_31.pdf.

[11] Kimura, H. and Kai, J., 1984. Phase change stability of CaCl2.6H2O. Solar Energy 33(6), 557-563.